

FORTY-SEVEN MILKY WAY-SIZED, EXTREMELY DIFFUSE GALAXIES IN THE COMA CLUSTER

PIETER G. VAN DOKKUM¹, ROBERTO ABRAHAM², ALLISON MERRITT¹, JIELAI ZHANG², MARLA GEHA¹, AND CHARLIE CONROY³

ABSTRACT

We report the discovery of 47 low surface brightness objects in deep images of a $3^\circ \times 3^\circ$ field centered on the Coma cluster, obtained with the Dragonfly Telephoto Array. The objects have central surface brightness $\mu(g, 0)$ ranging from 24 – 26 mag arcsec⁻² and effective radii $r_{\text{eff}} = 3'' - 10''$, as measured from archival Canada France Hawaii Telescope images. From their spatial distribution we infer that most or all of the objects are galaxies in the Coma cluster. This relatively large distance is surprising as it implies that the galaxies are very large: with $r_{\text{eff}} = 1.5 \text{ kpc} - 4.6 \text{ kpc}$ their sizes are similar to those of L_* galaxies even though their median stellar mass is only $\sim 6 \times 10^7 M_\odot$. The galaxies are relatively red and round, with $\langle g-i \rangle = 0.8$ and $\langle b/a \rangle = 0.74$. One of the 47 galaxies is fortuitously covered by a deep Hubble Space Telescope ACS observation. The ACS imaging shows a large spheroidal object with a central surface brightness $\mu_{475} = 25.8 \text{ mag arcsec}^{-2}$, a Sersic index $n = 0.6$, and an effective radius of $7''$, corresponding to 3.4 kpc at the distance of Coma. The galaxy is not resolved into stars, consistent with expectations for a Coma cluster object. We speculate that these “ultra-diffuse galaxies” (UDGs) may have lost their gas supply at early times, possibly resulting in very high dark matter fractions.

Keywords: galaxies: clusters: individual (Coma) — galaxies: evolution — galaxies: structure

1. INTRODUCTION

While there have been tremendous advances in deep, high resolution imaging surveys over the past decades (e.g., Scoville et al. 2007; Heymans et al. 2012), the low surface brightness sky remains relatively unexplored. The Dragonfly Telephoto Array (Abraham & van Dokkum 2014) was developed with the specific aim of detecting low surface brightness emission. It is comprised of eight Canon 400 mm f/2.8 II telephoto lenses which all image the same part of the sky, forming what is effectively a 40 cm f/1.0 refractor. Four of the lenses are equipped with an SDSS g filter and four with an SDSS r filter. The lenses are attached to cameras that provide an instantaneous field of view of $2.6^\circ \times 1.9^\circ$, sampled with $2''8$ pixels.

The main science program of Dragonfly is a deep imaging survey of a sample of nearby galaxies (see van Dokkum, Abraham, & Merritt 2014; Merritt, van Dokkum, & Abraham 2014). In the late Spring of 2014 we interrupted this survey to observe the Coma cluster. The main goal of the Coma observation is to accurately measure the luminosity and color of the intra-cluster light (ICL). We are also looking for streams and tidal features, inspired by the beautiful deep imaging of the Virgo cluster of Mihos et al. (2005).

A visual inspection of the reduced images revealed a large number of faint, spatially-resolved objects. The nature of these objects was not immediately obvious, as they are not listed in existing catalogs of faint galaxies in the Coma cluster (e.g., Ulmer et al. 1996; Adami et al. 2006). Furthermore, they seemed to be too large to be part of the cluster: typical dwarf galaxies have effective radii of a few hundred parsecs, which corresponds to much less than a Dragonfly pixel at the distance of Coma ($D_A = 98 \text{ Mpc}$; $D_L = 103 \text{ Mpc}$).⁴

Expecting that the objects would turn out to be isolated dwarf galaxies in the foreground of the cluster we decided

to perform a (mostly) objective selection with the aid of Sloan Digital Sky Survey (SDSS) and archival Canada France Hawaii Telescope (CFHT) data, as described in the next Section. Surprisingly, as we show below, the objects turn out to be associated with the Coma cluster after all, and represent a class of very large, very diffuse galaxies. Only a handful of similar objects were known from previous studies (Impey, Bothun, & Malin 1988; Bothun, Impey, & Malin 1991; Dalcanton et al. 1997).

2. IDENTIFICATION

2.1. Candidates in the Dragonfly Data

The Coma cluster was observed for 26 hrs, obtained over 25 nights in the period March – May 2014. The images were reduced using standard techniques, as described in van Dokkum et al. (2014) and Merritt et al. (2014), and projected onto a common astrometric frame with $2''0$ pixels. Owing to large dithers between individual exposures the final g and r images span $3.^\circ33 \times 3.^\circ33$, centered on $\alpha = 12^h59^m48.8^s$, $\delta = 27^\circ58'51''$. The FWHM image quality varies somewhat over the field, but is typically $\approx 6''$. The limiting depths in the images depend on the spatial scale; on the $10''$ scales relevant for this paper the 1σ limits are $\mu(g) \sim 29.3 \text{ mag arcsec}^{-2}$ and $\mu(r) \sim 28.6 \text{ mag arcsec}^{-2}$.

We used SExtractor (Bertin & Arnouts 1996) to create an initial catalog of 102,209 objects in the Dragonfly field. The g and r images were summed to increase the S/N ratio in the detection image. For each object two magnitudes were measured: one based on the flux in SExtractor’s “AUTO” aperture, and one in an aperture with a fixed diameter of $6''$. Objects were flagged as possible low surface brightness galaxies if their aperture magnitude is in the range $20 < AB < 23$ and the difference between the AUTO and aperture magnitude exceeds 1.8. The latter criterion rejects isolated stars and compact galaxies, leaving 6624 objects that are faint and extended at the Dragonfly resolution.

2.2. Rejection Using SDSS and CFHT

The vast majority of the 6624 objects are not low surface brightness galaxies but groups of neighboring galaxies, or

¹ Department of Astronomy, Yale University, New Haven, CT 06511, USA

² Department of Astronomy, University of Toronto, Toronto, Canada

³ Harvard-Smithsonian Center for Astrophysics, 60 Garden St., Cambridge, MA, USA

⁴ Assuming $c_z = 7090 \text{ km s}^{-1}$ (Geller, Diaferio, & Kurtz 1999) and a Hubble constant of $70 \text{ km s}^{-1} \text{ Mpc}^{-1}$.

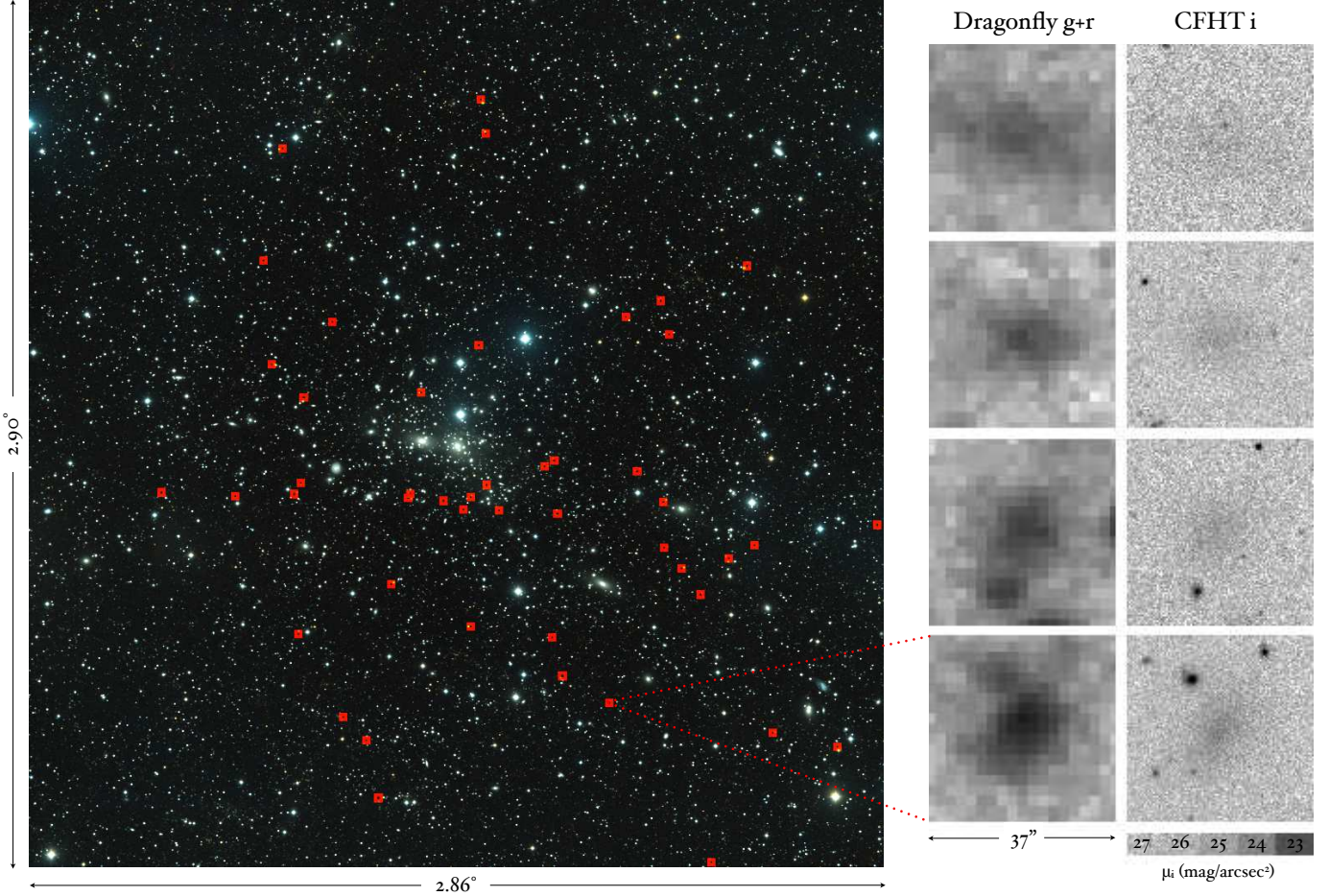


Figure 1. Main panel: spatial distribution of the newly discovered galaxies, projected on a color image of the Coma cluster created from the Dragonfly g and r images. Only the $2^{\circ}86 \times 2^{\circ}90$ area that is covered by CFHT imaging is shown. Panels at right: typical examples of the galaxies, spanning a range in brightness.

stars and galaxies, that are single objects at the Dragonfly resolution. We removed most of these by requiring that there is no object in the SDSS catalog within $4''$ of the Dragonfly position, leaving 344 candidates.

The SDSS imaging does not have sufficient depth and spatial resolution to identify faint groups of galaxies. We obtained CFHT imaging of the Coma field from the Canadian Astronomy Data Centre. A $3^{\circ} \times 3^{\circ}$ field was imaged with a 9-pointing mosaic, in the g and i bands (Head et al. 2014). Exposure times were short, at 300 s per pointing per filter, but the image quality ($\text{FWHM} \approx 0''.8$) and sampling ($0''.186 \text{ pixel}^{-1}$) are far superior to the Dragonfly and SDSS imaging. We created $37'' \times 37''$ cutouts of all 344 candidates and used SExtractor to identify cases where multiple moderately bright ($i < 22.5$) objects are detected within $7''$ of the Dragonfly position. This step left 186 objects which were inspected by eye. Of these, 139 were rejected, with most turning out to be clumps of multiple objects fainter than the $i = 22.5$ limit.

2.3. A Population of Large, Diffuse Galaxies

We are left with 47 objects, listed in Table 1, that are clearly detected in the Dragonfly imaging, are spatially-extended, are not detected in the SDSS, and do not resolve into multiple objects in the higher resolution CFHT data. Four typical examples spanning a range of apparent brightness are shown in

Fig. 1. The galaxies are clearly detected but barely resolved in the Dragonfly data, and very faint, fuzzy blobs in the CFHT data.

We had expected that the objects would be randomly distributed in the $3^{\circ} \times 3^{\circ}$ field that has both Dragonfly and CFHT coverage, as their apparent sizes seemed too large for a distance of 100 Mpc. However, as shown in Fig. 1 they are strongly clustered toward the center of the image. A Monte Carlo implementation of the Clark-Evans test gives a probability of 0.04% that the distribution is spatially-random. Moreover, the apparent East-West elongation of the distribution is similar to that of confirmed Coma cluster members (e.g., Doi et al. 1995). We conclude that most or all of the low surface brightness galaxies are, in fact, at the distance of the Coma cluster and are resolved in the Dragonfly data because they are intrinsically very large. As we show in § 4 this conclusion is supported by Hubble Space Telescope ACS imaging of one of the galaxies.

3. PROPERTIES

3.1. Structure

We used GALFIT (Peng et al. 2002) to measure structural parameters of the galaxies from the CFHT images. The fits were performed on the summed $g+i$ images, with neighboring objects masked. To increase the stability of the fits the

Sersic index and sky background were not allowed to vary. All galaxies were fit three times, with the Sersic index held fixed at $n = 0.5$, $n = 1$, and $n = 1.5$. The average χ^2 is lowest for $n = 1$ (exponential), but for individual galaxies the three fits are generally equally good. We therefore use the $n = 1$ results for all objects and determine the uncertainties in the structural parameters of individual galaxies from the full range of fits. Three examples of fits are shown in Fig. 2. Forty-six galaxies were successfully fit; the S/N ratio of one object (DF27) is too low for a stable fit.

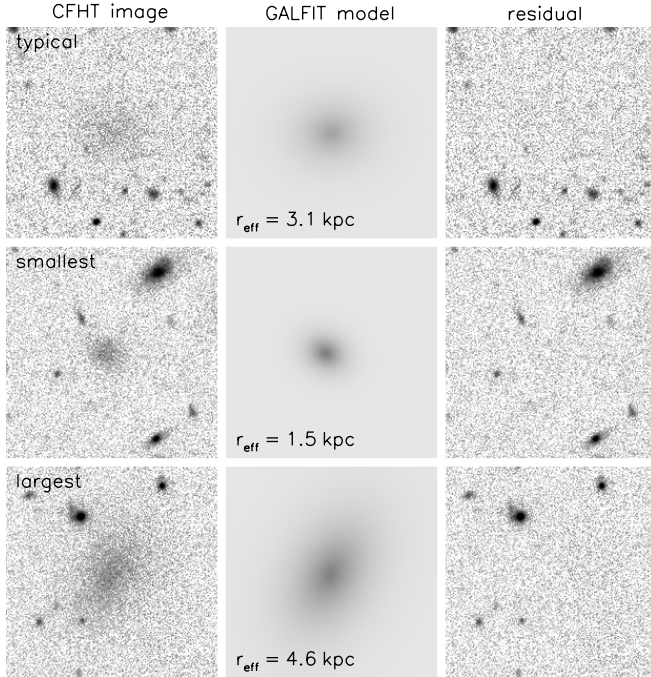


Figure 2. Examples of structural parameter fits to the CFHT data. Each panel spans $37'' \times 37''$. The left column shows the summed $g+i$ images, the middle column shows the best-fitting GALFIT models (with $n = 1$), and the right column shows the residuals from the fits. The size and surface brightness of the galaxy in the top (DF1) row are close to the median of the sample. The middle row shows the smallest galaxy in the sample (DF43), and the bottom row shows the largest (DF44).

The distribution of the galaxies in the surface brightness – size plane is shown in Fig. 3, under the assumption that they are all at the distance of the Coma cluster. The central surface brightnesses, calculated from the circularized effective radii and the total fit magnitudes, range from $\mu(g, 0) = 24\text{--}26$ mag arcsec $^{-2}$. The effective radii, measured along the major axis, range from 1.5 kpc to 4.5 kpc. At fixed surface brightness the newly found galaxies are much larger than typical dwarf elliptical galaxies in the Virgo cluster (open circles; Gavazzi et al. 2005). The median central surface brightness $\langle \mu(g, 0) \rangle = 25.0$ mag arcsec $^{-2}$ (≈ 25.4 mag arcsec $^{-2}$ in the B band) and the median effective radius $\langle r_{\text{eff}} \rangle = 2.8$ kpc. An interesting point of comparison is the disk of the Milky Way. Bovy & Rix (2013) derive a mass-weighted exponential scale length of 2.15 ± 0.14 kpc, corresponding to $r_{\text{eff}} = 3.6$ kpc. Twelve of the newly found objects are larger than this, although for individual objects the difference is typically not significant. We note that the gap between SDSS and the Dragonfly data in Fig. 3 is due to the selection limits of the sur-

veys. The newly found galaxies are simply the low surface brightness, large size extension of the general galaxy population, and samples such as that of Thompson & Gregory (1993) would fill in the gap.

The axis ratio distribution is shown in the right panel of Fig. 3. The galaxies are remarkably round, with a median axis ratio of 0.74. We note that there is no obvious selection effect against inclined disks, as the galaxies are barely resolved in the Dragonfly data. Randomly oriented thin disks would have a uniform b/a distribution, and this can be ruled out.

3.2. Stellar Content

The median absolute g band magnitude $\langle M_g \rangle = -14.3$. The average color of the galaxies $\langle g-i \rangle = 0.8 \pm 0.1$, as measured from stacks of the CFHT g and i images. Their colors are similar to those of the reddest Milky Way globular clusters (Vanderbeke et al. 2014), and consistent with an extrapolation of the red sequence of early-type galaxies in Coma (Gavazzi et al. 2010). The observed color is consistent with a passively evolving stellar population with a low metallicity and/or a relatively young age. For example, the Conroy, Gunn, & White (2009) models predict $g-i = 0.8$ for an age of 7 Gyr and $[\text{Fe}/\text{H}] = -1.4$, and for an age of 4 Gyr and $[\text{Fe}/\text{H}] = -0.8$ (see also Michielsen et al. 2008).

From the absolute magnitudes and colors we can estimate the stellar masses of the galaxies. The absolute magnitudes range from $-16.0 \leq M_g \leq -12.5$; using Eq. 8 in Taylor et al. (2011) with $g-i = 0.8$ we find that the galaxies have stellar masses in the range $1 \times 10^7 M_\odot - 3 \times 10^8 M_\odot$. The median stellar mass $\langle M_{\text{star}} \rangle \sim 6 \times 10^7 M_\odot$, and the median stellar density within the effective radius is $\sim 5 \times 10^5 M_\odot \text{ kpc}^{-3}$.

4. DEEP HST/ACS IMAGING

We searched the HST Archive for serendipitous observations of the newly found galaxies. Three of the 47 galaxies have been observed by HST. Two of the observations are short (200 s – 300 s) WFPC2 exposures, which show only hints of the objects. The third comprises 8-orbit, multi-band ACS imaging of DF17, whose properties are close to the median of the sample. The ACS data include g_{475} , V_{606} , and I_{814} parallels to a Cepheid program with the WFC3/UVIS camera (GO-12476, PI: Cook; Macri et al. 2013). The data were obtained from the archive and reduced using standard techniques (van Dokkum 2001).

A color image, created from the V_{606} and I_{814} images, is shown in Fig. 4. DF17 is large and spheroidal and does not have obvious spiral arms, star forming regions, or tidal features. We fit the ACS data with a Sersic profile, leaving all parameters free. The best fitting parameters are $r_{\text{eff}} = 7''.0$, $n = 0.6$, $\mu_{475} = 25.8$, and $b/a = 0.71$. The effective radius, surface brightness, and axis ratio are in excellent agreement with the $n = 0.5$ fit to the CFHT image.

The fact that the galaxy is not resolved into stars implies a lower limit to its distance. We created model images of DF17, following the methodology described in van Dokkum & Conroy (2014). Stars were drawn randomly from a Poisson distribution, weighted by their expected frequency in a 10 Gyr old stellar population with a metallicity $[\text{Fe}/\text{H}] = -1.6$. This stellar population reproduces the observed $V_{606} - I_{814}$ color ($V_{606} - I_{814} = 0.40$). The models are constrained to reproduce the observed 2D light distribution of DF17 and its observed total magnitude of $I_{814} = 19.3$, with the distance as the only free parameter. The model images were convolved with the

Table 1
Positions and Properties

Id	RA (J2000)	Dec (J2000)	$\mu(g, 0)$ (mag arcsec ⁻²)	r_{eff} (kpc)	M_g (mag)	b/a
DF1	12 ^h 59 ^m 14.1 ^s	29° 07' 16"	25.1 ^{+0.5} _{-0.5}	3.1 ^{+0.9} _{-0.6}	-14.6 ^{+0.3} _{-0.2}	0.82 ± 0.03
DF2	12 ^h 59 ^m 09.5 ^s	29° 00' 25"	24.4 ^{+0.6} _{-0.6}	2.1 ^{+0.6} _{-0.4}	-14.3 ^{+0.2} _{-0.2}	0.71 ± 0.03
DF3	13 ^h 02 ^m 16.5 ^s	28° 57' 17"	24.5 ^{+0.5} _{-0.5}	2.9 ^{+0.8} _{-0.7}	-14.2 ^{+0.3} _{-0.2}	0.40 ± 0.04
DF4	13 ^h 02 ^m 33.4 ^s	28° 34' 51"	25.7 ^{+0.6} _{-0.6}	3.9 ^{+1.0} _{-0.5}	-14.3 ^{+0.2} _{-0.2}	0.71 ± 0.03
DF5	12 ^h 55 ^m 10.5 ^s	28° 33' 32"	24.9 ^{+0.6} _{-0.6}	1.8 ^{+0.4} _{-0.4}	-13.5 ^{+0.2} _{-0.2}	0.71 ± 0.03
DF6	12 ^h 56 ^m 29.7 ^s	28° 26' 40"	25.5 ^{+0.5} _{-0.5}	4.4 ^{+1.6} _{-1.1}	-14.3 ^{+0.4} _{-0.3}	0.47 ± 0.03
DF7	12 ^h 57 ^m 01.7 ^s	28° 23' 25"	24.4 ^{+0.5} _{-0.5}	4.3 ^{+1.4} _{-0.8}	-16.0 ^{+0.2} _{-0.2}	0.76 ± 0.03
DF8	13 ^h 01 ^m 30.4 ^s	28° 22' 28"	25.4 ^{+0.5} _{-0.5}	4.4 ^{+1.5} _{-0.9}	-14.9 ^{+0.3} _{-0.3}	0.73 ± 0.05
DF9	12 ^h 56 ^m 22.8 ^s	28° 19' 53"	25.6 ^{+0.7} _{-0.7}	2.8 ^{+0.5} _{-0.4}	-14.0 ^{+0.1} _{-0.1}	0.92 ± 0.03
DF10	12 ^h 59 ^m 16.3 ^s	28° 17' 51"	24.4 ^{+0.6} _{-0.6}	2.4 ^{+0.6} _{-0.4}	-14.7 ^{+0.2} _{-0.2}	0.83 ± 0.03
DF11	13 ^h 02 ^m 25.5 ^s	28° 13' 58"	24.2 ^{+0.6} _{-0.6}	2.1 ^{+0.4} _{-0.3}	-14.8 ^{+0.2} _{-0.1}	0.98 ± 0.03
DF12	13 ^h 00 ^m 09.1 ^s	28° 08' 27"	25.2 ^{+0.6} _{-0.6}	2.6 ^{+0.6} _{-0.9}	-14.1 ^{+0.5} _{-0.2}	0.88 ± 0.03
DF13	13 ^h 01 ^m 56.2 ^s	28° 07' 23"	25.3 ^{+0.6} _{-0.6}	2.2 ^{+0.6} _{-0.5}	-13.7 ^{+0.3} _{-0.2}	0.83 ± 0.03
DF14	12 ^h 58 ^m 07.8 ^s	27° 54' 46"	25.3 ^{+0.7} _{-0.7}	3.8 ^{+0.8} _{-0.1}	-14.4 ^{+0.1} _{-0.1}	0.51 ± 0.07
DF15	12 ^h 58 ^m 16.3 ^s	27° 53' 29"	25.5 ^{+0.1} _{-0.1}	4.0 ^{+5.5} _{-0.1}	-14.9 ^{+0.1} _{-0.4}	0.99 ± 0.29
DF16	12 ^h 56 ^m 52.4 ^s	27° 52' 29"	24.8 ^{+0.8} _{-0.8}	1.5 ^{+0.1} _{-0.2}	-13.2 ^{+0.2} _{-0.1}	0.82 ± 0.10
DF17	13 ^h 01 ^m 58.3 ^s	27° 50' 11"	25.1 ^{+0.5} _{-0.5}	4.4 ^{+1.5} _{-0.9}	-15.2 ^{+0.3} _{-0.2}	0.71 ± 0.03
DF18	12 ^h 59 ^m 09.3 ^s	27° 49' 48"	25.5 ^{+0.6} _{-0.6}	2.8 ^{+0.6} _{-0.5}	-13.4 ^{+0.2} _{-0.1}	0.47 ± 0.03
DF19	13 ^h 04 ^m 05.1 ^s	27° 48' 05"	25.9 ^{+0.5} _{-0.5}	4.4 ^{+1.6} _{-0.9}	-14.5 ^{+0.3} _{-0.3}	0.78 ± 0.03
DF20	13 ^h 00 ^m 18.9 ^s	27° 48' 06"	25.5 ^{+0.8} _{-0.8}	2.3 ^{+0.3} _{-0.1}	-13.0 ^{+0.1} _{-0.1}	0.53 ± 0.11
DF21	13 ^h 02 ^m 04.1 ^s	27° 47' 55"	23.5 ^{+0.7} _{-0.7}	1.5 ^{+0.3} _{-0.2}	-14.6 ^{+0.2} _{-0.1}	0.82 ± 0.03
DF22	13 ^h 02 ^m 57.8 ^s	27° 47' 25"	25.1 ^{+0.6} _{-0.6}	2.1 ^{+0.4} _{-0.3}	-13.8 ^{+0.2} _{-0.1}	0.84 ± 0.03
DF23	12 ^h 59 ^m 23.8 ^s	27° 47' 27"	24.8 ^{+0.6} _{-0.6}	2.3 ^{+0.5} _{-0.3}	-14.3 ^{+0.2} _{-0.2}	0.89 ± 0.03
DF24	12 ^h 56 ^m 28.9 ^s	27° 46' 19"	25.2 ^{+0.7} _{-0.7}	1.8 ^{+0.4} _{-0.4}	-12.5 ^{+0.2} _{-0.2}	0.38 ± 0.03
DF25	12 ^h 59 ^m 48.7 ^s	27° 46' 39"	25.2 ^{+0.5} _{-0.5}	4.4 ^{+1.4} _{-0.7}	-14.5 ^{+0.2} _{-0.2}	0.43 ± 0.03
DF26	13 ^h 00 ^m 20.6 ^s	27° 47' 13"	24.1 ^{+0.6} _{-0.6}	3.3 ^{+0.8} _{-0.4}	-15.4 ^{+0.2} _{-0.2}	0.63 ± 0.03
DF27	12 ^h 58 ^m 57.3 ^s	27° 44' 39"	≥ 26.5
DF28	12 ^h 59 ^m 30.4 ^s	27° 44' 50"	24.4 ^{+0.6} _{-0.6}	2.7 ^{+0.6} _{-0.4}	-14.9 ^{+0.2} _{-0.2}	0.79 ± 0.03
DF29	12 ^h 58 ^m 05.0 ^s	27° 43' 59"	25.3 ^{+0.2} _{-0.2}	3.1 ^{+1.6} _{-0.1}	-14.6 ^{+0.1} _{-0.1}	0.99 ± 0.13
DF30	12 ^h 53 ^m 15.1 ^s	27° 41' 15"	24.4 ^{+0.5} _{-0.5}	3.2 ^{+0.9} _{-0.6}	-15.2 ^{+0.2} _{-0.2}	0.70 ± 0.03
DF31	12 ^h 55 ^m 06.2 ^s	27° 37' 27"	25.0 ^{+0.5} _{-0.5}	2.5 ^{+0.7} _{-0.6}	-14.1 ^{+0.3} _{-0.2}	0.75 ± 0.03
DF32	12 ^h 56 ^m 28.4 ^s	27° 37' 06"	24.8 ^{+0.6} _{-0.6}	2.8 ^{+0.6} _{-0.3}	-14.2 ^{+0.1} _{-0.1}	0.52 ± 0.03
DF33	12 ^h 55 ^m 30.1 ^s	27° 34' 50"	25.1 ^{+0.7} _{-0.7}	1.9 ^{+0.2} _{-0.1}	-13.4 ^{+0.1} _{-0.1}	0.69 ± 0.03
DF34	12 ^h 56 ^m 12.9 ^s	27° 32' 52"	26.0 ^{+0.6} _{-0.6}	3.4 ^{+0.5} _{-0.4}	-13.6 ^{+0.1} _{-0.1}	0.66 ± 0.03
DF35	13 ^h 00 ^m 35.7 ^s	27° 29' 51"	25.6 ^{+0.4} _{-0.4}	2.7 ^{+1.0} _{-0.3}	-13.9 ^{+0.2} _{-0.2}	0.89 ± 0.09
DF36	12 ^h 55 ^m 55.4 ^s	27° 27' 36"	25.0 ^{+0.6} _{-0.6}	2.6 ^{+1.0} _{-0.4}	-14.3 ^{+0.3} _{-0.4}	0.80 ± 0.14
DF37	12 ^h 59 ^m 23.6 ^s	27° 21' 22"	24.5 ^{+0.7} _{-0.7}	1.5 ^{+0.3} _{-0.2}	-13.7 ^{+0.2} _{-0.2}	0.83 ± 0.03
DF38	13 ^h 02 ^m 00.1 ^s	27° 19' 51"	24.2 ^{+0.6} _{-0.6}	1.8 ^{+0.4} _{-0.3}	-14.3 ^{+0.2} _{-0.1}	0.84 ± 0.03
DF39	12 ^h 58 ^m 10.4 ^s	27° 19' 11"	25.5 ^{+0.5} _{-0.5}	4.0 ^{+1.3} _{-0.7}	-14.7 ^{+0.2} _{-0.2}	0.77 ± 0.05
DF40	12 ^h 58 ^m 01.1 ^s	27° 11' 26"	24.6 ^{+0.6} _{-0.6}	2.9 ^{+0.7} _{-0.5}	-14.6 ^{+0.2} _{-0.2}	0.56 ± 0.03
DF41	12 ^h 57 ^m 19.0 ^s	27° 05' 56"	24.9 ^{+0.5} _{-0.5}	3.4 ^{+0.9} _{-0.5}	-14.7 ^{+0.1} _{-0.1}	0.64 ± 0.03
DF42	13 ^h 01 ^m 19.1 ^s	27° 03' 15"	25.0 ^{+0.6} _{-0.6}	2.9 ^{+0.6} _{-0.4}	-14.1 ^{+0.1} _{-0.1}	0.52 ± 0.03
DF43	12 ^h 54 ^m 51.4 ^s	26° 59' 46"	24.2 ^{+0.8} _{-0.8}	1.5 ^{+0.2} _{-0.2}	-13.8 ^{+0.2} _{-0.2}	0.82 ± 0.10
DF44	13 ^h 00 ^m 58.0 ^s	26° 58' 35"	24.5 ^{+0.5} _{-0.5}	4.6 ^{+1.5} _{-0.8}	-15.7 ^{+0.2} _{-0.2}	0.65 ± 0.03
DF45	12 ^h 53 ^m 53.7 ^s	26° 56' 48"	24.4 ^{+0.5} _{-0.5}	1.9 ^{+0.6} _{-0.4}	-14.2 ^{+0.2} _{-0.2}	0.80 ± 0.03
DF46	13 ^h 00 ^m 47.3 ^s	26° 46' 59"	25.4 ^{+0.6} _{-0.6}	3.4 ^{+1.0} _{-0.6}	-14.4 ^{+0.2} _{-0.2}	0.74 ± 0.04
DF47	12 ^h 55 ^m 48.1 ^s	26° 33' 53"	25.5 ^{+0.5} _{-0.5}	4.2 ^{+1.4} _{-0.7}	-14.6 ^{+0.1} _{-0.2}	0.66 ± 0.04

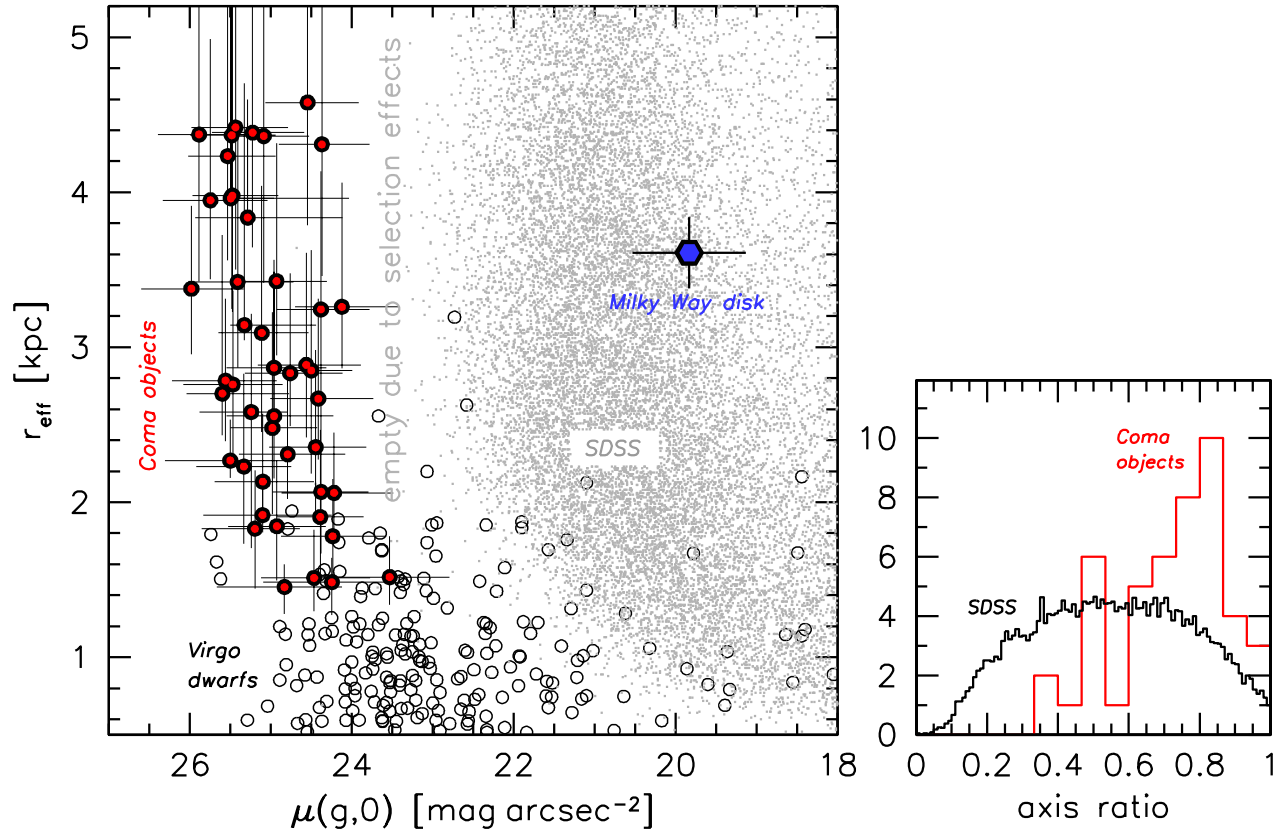


Figure 3. Main panel: Location of the newly found galaxies in the effective radius – central surface brightness plane, compared to galaxies at $0.02 < z < 0.03$ in the SDSS (Simard et al. 2011), early-type galaxies in the Virgo cluster (Gavazzi et al. 2005), and the disk of the Milky Way (Bovy & Rix 2013). Right panel: Axis ratio distribution compared to that of similar-sized SDSS galaxies.

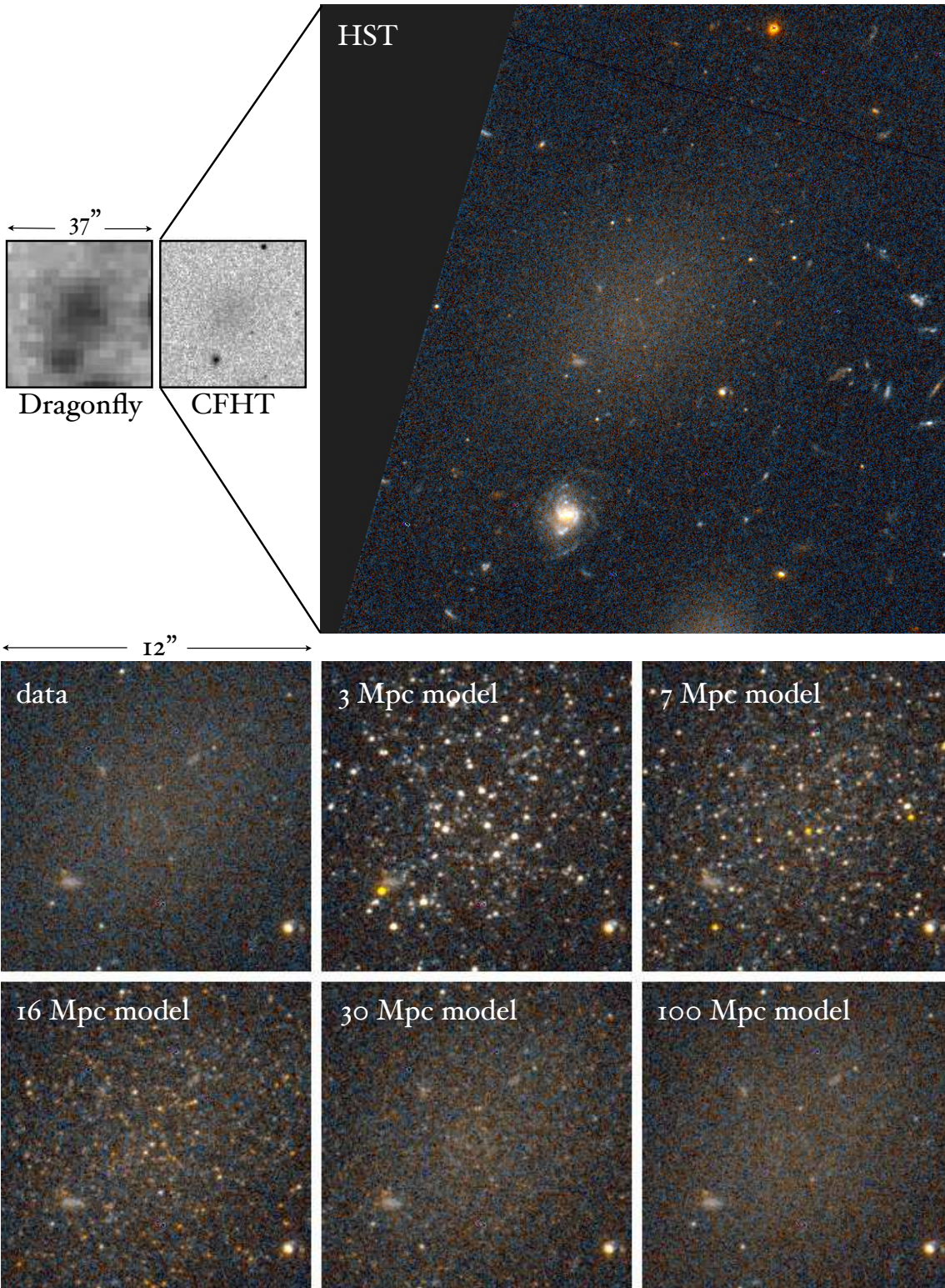


Figure 4. One of the galaxies, DF17, has been observed with ACS on HST. The main panel shows a color image created from the V_{606} and I_{814} ACS images. The galaxy is smooth, red, spheroidal, and is not resolved into stars. The bottom panels show the expected appearance of the galaxy for different distances (see text). The ACS data are consistent with the Coma distance of ≈ 100 Mpc.

ACS PSF and placed in the ACS image, after subtracting the best-fitting GALFIT model of the galaxy.

The results are shown in the bottom panels of Fig. 4. Out well beyond the Virgo cluster (16 Mpc) the ACS camera easily resolves individual stars in low surface brightness galaxies, as also shown by Caldwell (2006). Only at distances $\gtrsim 50$ Mpc do the models take on the same smooth appearance as the data, and we conclude that the ACS observations support the interpretation that the galaxies are associated with the Coma cluster. The effective radius of DF17 is then 3.4 kpc, almost identical to that of the disk of the Milky Way.

5. DISCUSSION

We have identified a significant population of low surface brightness, red, nearly round objects in a wide field centered on the Coma cluster. Based on their spatial distribution and the analysis of one example observed with ACS we infer that most or all of the objects are associated with Coma. Their inferred sizes are similar to those of L_* galaxies and the disk of the Milky Way, even though their stellar masses are a factor of $\sim 10^3$ lower.

The galaxies do not resemble “classical” low surface brightness galaxies (LSBs) such as those described by, e.g., van der Hulst et al. (1993), Bothun, Impey, & McGaugh (1997), and van den Hoek et al. (2000). Typical LSBs have blue, gas-rich disks, and are thought to be normal spiral galaxies with a low stellar content and low star formation rate for their rotation velocity (see, e.g., Schombert, McGaugh, & Maciel 2013, and references therein). They are also significantly brighter than the objects found in this paper: the lowest surface brightness object in the compilation of Bothun et al. (1997) has $\mu(0, B) \approx 24.0$ mag arcsec $^{-2}$, corresponding to $\mu(0, g) \approx 23.6$ mag arcsec $^{-2}$. Many have bulges; for example, Malin I has a central surface brightness $\lesssim 16$ mag arcsec $^{-2}$ if its bulge is taken into account (Lelli, Fraternali, & Sancisi 2010).

Visually and structurally, the newly found galaxies are more similar to dwarf spheroidal galaxies such as those found in the Local Group, around M101, and in the Virgo and Coma clusters than to classical LSBs: they have similar Sersic indices, axis ratios, and surface brightness (e.g., Thompson & Gregory 1993; Geha, Guhathakurta, & van der Marel 2003; Gavazzi et al. 2005; McConnachie 2012; Merritt et al. 2014; Toloba et al. 2014). However, the term “dwarf” is not appropriate for these large objects. Dwarf spheroidals have typical sizes of a few hundred pc (e.g., McConnachie 2012; Lieder et al. 2012), and in the Local Group and other nearby groups only a few have an effective radius exceeding 1 kpc (e.g. Kim et al. 2011; McConnachie 2012; Chiboucas et al. 2013; Merritt et al. 2014). The largest known low luminosity Local Group galaxy is And XIX, with a size of 1.6 kpc (McConnachie et al. 2008). The Coma objects are much larger, with sizes typical of $\sim L_*$ spiral and elliptical galaxies (e.g., Shen et al. 2003).

The closest analogs to the Coma objects are several very large low surface brightness objects in the Virgo and Fornax clusters, first identified by Impey et al. (1988). There are four galaxies in the Impey et al. sample with central surface brightness $\gtrsim 25$ mag arcsec $^{-2}$ and $r_{\text{eff}} > 2.5$ kpc; the largest of these, V1L5 and V4L7, have $r_{\text{eff}} = 3.7$ kpc. As the Impey et al. survey area is $4\times$ smaller than ours the number of such galaxies in Virgo and Coma could be similar. Although the distances to these particular objects are not confirmed, Caldwell (2006) used HST/ACS imaging to show that at least one galaxy with



Figure 5. Central $0^\circ 89 \times 0^\circ 70$ (1.6 Mpc \times 1.2 Mpc) of the Dragonfly image shown in Fig. 1. The newly found galaxies appear to avoid the region where ICL is detected.

a central surface brightness of $\mu(g, 0) \approx 27.2$ and an effective radius of 1.5 kpc is part of the Virgo cluster. We propose the term “ultra-diffuse galaxies”, or UDGs, for galaxies with $r_e \gtrsim 1.5$ kpc and $\mu(g, 0) \gtrsim 24$ mag arcsec $^{-2}$. We stress that this term does not imply that these objects are distinct from the general galaxy population; these are simply the largest and most diffuse objects in a continuous distribution.

As shown in Fig. 5 no UDGs are found in the central regions of the cluster, consistent with earlier results for slightly brighter diffuse spheroidals in Coma (Thompson et al. 1993). This could mean that they are only able to survive at large radii (see, e.g., Bothun et al. 1991; Gregg & West 1998; Martel, Barai, & Brito 2012). We can estimate what the mass of the galaxies needs to be to survive a passage within ~ 300 kpc of the core of the cluster, which is where the closest-in UDGs are located. The criterion for survival is that the total mass m_{tot} within the tidal radius $r_{\text{tide}} = 2r_e = 6$ kpc is at least $m_{\text{tot}} > 3M(r_{\text{tide}}/R)^3$, with M the mass of the cluster within radius R . Using the mass profile of Abell 2667 (Newman et al. 2013) as a proxy for that of Coma, we find $m_{\text{tot}} \gtrsim 3 \times 10^9 M_\odot$, or a dark matter fraction *within the tidal radius* of $\gtrsim 98\%$. We note that there may be UDGs closer to the cluster core, as crowding and the ICL limit our ability to detect them (see Ulmer et al. 1996; Adami et al. 2006, 2009).

It is not clear how UDGs were formed. It seems unlikely that they are the product of galaxy harassment (Moore et al. 1996) or tidal stirring (Mayer et al. 2001) of infalling galaxies: these processes tend to *shrink* galaxies, as the stars at larger radii are less bound than the stars at small radii (see, e.g., Mayer et al. 2001). A likely end-product of cluster-induced tidal effects are the ultra-compact dwarfs (Drinkwater et al. 2003), which have similar total luminosities and stellar masses as UDGs but stellar densities that are a factor of $\sim 10^7$ higher.⁵ We note, however, that the morphological evolution of infalling galaxies is difficult to predict, as it probably depends sensitively on the shape of the inner dark matter profile (e.g., Peñarrubia et al. 2010). An intriguing formation scenario is that UDGs are “failed” $\sim L_*$ galaxies, which lost

⁵ It is remarkable that both classes of objects exist in clusters at the same time.

their gas after forming their first generation(s) of stars at high redshift (by ram pressure stripping or other effects). If this is the case they may have very high dark matter fractions, which could also help explain their survival in the cluster. Future studies of these objects, as well as counterparts in other clusters and in the field (see Dalcanton et al. 1997), may shed more light on these issues.

We thank the anonymous referee for an excellent and constructive report. We also thank the staff at New Mexico Skies for their support and Nelson Caldwell for comments on the manuscript. Support from NSF grant AST-1312376 is gratefully acknowledged.

REFERENCES

- Abraham, R. G. & van Dokkum, P. G. 2014, *PASP*, 126, 55
- Adami, C., Pelló, R., Ulmer, M. P., Cuillandre, J. C., Durret, F., Mazure, A., Picat, J. P., & Scheidegger, R. 2009, *A&A*, 495, 407
- Adami, C., Scheidegger, R., Ulmer, M., Durret, F., Mazure, A., West, M. J., Conselice, C. J., Gregg, M., et al. 2006, *A&A*, 459, 679
- Bertin, E. & Arnouts, S. 1996, *A&AS*, 117, 393
- Bothun, G., Impey, C., & McGaugh, S. 1997, *PASP*, 109, 745
- Bothun, G. D., Impey, C. D., & Malin, D. F. 1991, *ApJ*, 376, 404
- Bovy, J. & Rix, H.-W. 2013, *ApJ*, 779, 115
- Caldwell, N. 2006, *ApJ*, 651, 822
- Chiboucas, K., Jacobs, B. A., Tully, R. B., & Karachentsev, I. D. 2013, *AJ*, 146, 126
- Conroy, C., Gunn, J. E., & White, M. 2009, *ApJ*, 699, 486
- Dalcanton, J. J., Spergel, D. N., Gunn, J. E., Schmidt, M., & Schneider, D. P. 1997, *AJ*, 114, 635
- Doi, M., Fukugita, M., Okamura, S., & Turner, E. L. 1995, *AJ*, 109, 1490
- Drinkwater, M. J., Gregg, M. D., Hilker, M., Bekki, K., Couch, W. J., Ferguson, H. C., Jones, J. B., & Phillipps, S. 2003, *Nature*, 423, 519
- Gavazzi, G., Donati, A., Cucciati, O., Sabatini, S., Boselli, A., Davies, J., & Zibetti, S. 2005, *A&A*, 430, 411
- Gavazzi, G., Fumagalli, M., Cucciati, O., & Boselli, A. 2010, *A&A*, 517, A73
- Geha, M., Guhathakurta, P., & van der Marel, R. P. 2003, *AJ*, 126, 1794
- Geller, M. J., Diaferio, A., & Kurtz, M. J. 1999, *ApJ*, 517, L23
- Gregg, M. D. & West, M. J. 1998, *Nature*, 396, 549
- Head, J. T. C. G., Lucey, J. R., Hudson, M. J., & Smith, R. J. 2014, *MNRAS*, 440, 1690
- Heymans, C., Van Waerbeke, L., Miller, L., Erben, T., Hildebrandt, H., Hoekstra, H., Kitching, T. D., Mellier, Y., et al. 2012, *MNRAS*, 427, 146
- Impey, C., Bothun, G., & Malin, D. 1988, *ApJ*, 330, 634
- Kim, E., Kim, M., Hwang, N., Lee, M. G., Chun, M.-Y., & Ann, H. B. 2011, *MNRAS*, 412, 1881
- Lelli, F., Fraternali, F., & Sancisi, R. 2010, *A&A*, 516, A11
- Lieder, S., Lisker, T., Hilker, M., Misgeld, I., & Durrell, P. 2012, *A&A*, 538, A69
- Macri, L. M., Hoffmann, S. L., Cook, K. H., Gregg, M., Mould, J. R., Stetson, P. B., & Welch, D. L. 2013, in *American Astronomical Society Meeting Abstracts*, Vol. 221, American Astronomical Society Meeting Abstracts 221, 152.06
- Martel, H., Barai, P., & Brito, W. 2012, *ApJ*, 757, 48
- Mayer, L., Governato, F., Colpi, M., Moore, B., Quinn, T., Wadsley, J., Stadel, J., & Lake, G. 2001, *ApJ*, 559, 754
- McConnachie, A. W. 2012, *AJ*, 144, 4
- McConnachie, A. W., Huxor, A., Martin, N. F., Irwin, M. J., Chapman, S. C., Fahlman, G., Ferguson, A. M. N., Ibata, R. A., et al. 2008, *ApJ*, 688, 1009
- Merritt, A., van Dokkum, P., & Abraham, R. 2014, *ApJ*, 787, L37
- Michielsen, D., Boselli, A., Conselice, C. J., Toloba, E., Whiley, I. M., Aragón-Salamanca, A., Balcells, M., Cardiel, N., et al. 2008, *MNRAS*, 385, 1374
- Mihos, J. C., Harding, P., Feldmeier, J., & Morrison, H. 2005, *ApJ*, 631, L41
- Moore, B., Katz, N., Lake, G., Dressler, A., & Oemler, A. 1996, *Nature*, 379, 613
- Newman, A. B., Treu, T., Ellis, R. S., Sand, D. J., Nipoti, C., Richard, J., & Jullo, E. 2013, *ApJ*, 765, 24
- Peñarrubia, J., Benson, A. J., Walker, M. G., Gilmore, G., McConnachie, A. W., & Mayer, L. 2010, *MNRAS*, 406, 1290
- Peng, C. Y., Ho, L. C., Impey, C. D., & Rix, H.-W. 2002, *AJ*, 124, 266
- Schombert, J., McGaugh, S., & Maciel, T. 2013, *AJ*, 146, 41
- Scoville, N., Aussel, H., Brusa, M., Capak, P., Carollo, C. M., Elvis, M., Gialalisco, M., Guzzo, L., et al. 2007, *ApJS*, 172, 1
- Shen, S., Mo, H. J., White, S. D. M., Blanton, M. R., Kauffmann, G., Voges, W., Brinkmann, J., & Csabai, I. 2003, *MNRAS*, 343, 978
- Simard, L., Mendel, J. T., Patton, D. R., Ellison, S. L., & McConnachie, A. W. 2011, *ApJS*, 196, 11
- Taylor, E. N., Hopkins, A. M., Baldry, I. K., Brown, M. J. I., Driver, S. P., Kelvin, L. S., Hill, D. T., Robotham, A. S. G., et al. 2011, *MNRAS*, 418, 1587
- Thompson, L. A., & Gregory, S. A. 1993, *AJ*, 106, 2197
- Toloba, E., Guhathakurta, P., Boselli, A., Peletier, R., Emsellem, E., Lisker, T., van de Ven, G., Simon, J., et al. 2014, *ArXiv e-prints*
- Ulmer, M. P., Bernstein, G. M., Martin, D. R., Nichol, R. C., Pendleton, J. L., & Tyson, J. A. 1996, *AJ*, 112, 2517
- van den Hoek, L. B., de Blok, W. J. G., van der Hulst, J. M., & de Jong, T. 2000, *A&A*, 357, 397
- Vanderbeke, J., West, M. J., De Propriis, R., Peng, E. W., Blakeslee, J. P., Jordán, A., Coté, P., Gregg, M., et al. 2014, *MNRAS*, 437, 1734
- van der Hulst, J. M., Skillman, E. D., Smith, T. R., Bothun, G. D., McGaugh, S. S., & de Blok, W. J. G. 1993, *AJ*, 106, 548
- van Dokkum, P. & Conroy, C. 2014, *ArXiv e-prints*
- van Dokkum, P. G. 2001, *PASP*, 113, 1420
- van Dokkum, P. G., Abraham, R., & Merritt, A. 2014, *ApJ*, 782, L24